



HAL
open science

On-line spectroscopic study of brominated flame retardant extraction in supercritical CO₂

Dong Xia, Ange Maurice, Antoine Leybros, Jong-Min Lee, Agnès Grandjean,
Jean-Christophe Gabriel

► **To cite this version:**

Dong Xia, Ange Maurice, Antoine Leybros, Jong-Min Lee, Agnès Grandjean, et al.. On-line spectroscopic study of brominated flame retardant extraction in supercritical CO₂. *Chemosphere*, 2021, 263, pp.128282. 10.1016/j.chemosphere.2020.128282 . cea-02936108

HAL Id: cea-02936108

<https://cea.hal.science/cea-02936108>

Submitted on 11 Sep 2020

HAL is a multi-disciplinary open access archive for the deposit and dissemination of scientific research documents, whether they are published or not. The documents may come from teaching and research institutions in France or abroad, or from public or private research centers.

L'archive ouverte pluridisciplinaire **HAL**, est destinée au dépôt et à la diffusion de documents scientifiques de niveau recherche, publiés ou non, émanant des établissements d'enseignement et de recherche français ou étrangers, des laboratoires publics ou privés.

1 **On-Line Study of Flame Retardants Extraction in Supercritical CO₂**

2 Dong Xia^a, Ange Maurice^a, Antoine Leybros^b, Jong-Min Lee^{a,c}, Agnes Grandjean^b and Jean-Christophe P.

3 Gabriel^{a,d*}

4 ^a *Nanyang Technological University, Energy Research Institute @ NTU (ERI@N), SCARCE Laboratory,*

5 *637459, Singapore.*

6 ^b *CEA, DES, ISEC, DMRC, Univ Montpellier, Marcoule, France*

7 ^c *Nanyang Technological University, School of Chemical and Biomedical Engineering, 637459, Singapore.*

8 ^d *Université Paris-Saclay, CEA, CNRS, NIMBE, 91191, Gif-sur-Yvette, France.*

9 *Corresponding author. Jean-Christophe P. Gabriel

10 *E-mail address: Jean-christophe.gabriel@cea.fr / jgabriel@ntu.edu.sg*

11 **ABSTRACT**

12 Extraction of brominated flame retardants (BFRs) from polymers before disposal or recycling will alleviate
13 negative environmental effects and ensure safe usage of recycled products. Supercritical CO₂ is appealing as
14 solvent owing to its green properties but also challenging due to its limited solvation power towards polar
15 molecules. For a more comprehensive evaluation of supercritical extraction potentialities, we (i) developed an
16 on-line analytical technique compatible with both UV-vis and FTIR spectroscopies to enable kinetic and
17 thermodynamic studies; (ii) studied kinetic extraction of three conventional and two novel BFRs. Concentration
18 at saturation were determined by gravimetric method or X-ray fluorescence. When compared to UV-vis, FTIR
19 exhibited a higher applicability to follow BFR extraction's time-dependency binary and ternary systems. Faster
20 stirring speed, higher temperature, and finer particle size were found to accelerate overall extraction kinetics. In

21 binary systems, times required to achieve equilibrium for each BFR were less than 2 hours at 60 °C, 25 MPa and
22 1000 rpm. In ternary systems with the presence of cosolvent (water) or polymeric matrix, extraction kinetics
23 were found to slow down due to competitive dissolution and molecular diffusion within matrix. Mathematical
24 models derived from irreversible desorption and Fick's diffusion laws were applied to fit observed extraction
25 kinetics of BFRs with absolute average relative deviations lower than 5.7%, enabling us to identify the rate-
26 determining step. Our high solubilization rate coefficients measurements for BFRs proves that it can compensate
27 for their low solubility if one uses flowing supercritical CO₂.

28 *Keywords:* Extraction; Kinetic; Brominated Flame Retardant; Spectroscopy; Supercritical CO₂; On-line analysis

29 **1. Introduction**

30 Rapid development in polymer science over the past 70 years has led to the introduction of a tremendous
31 amount of polymeric materials into people's daily life ([Alaee, 2003](#)). To ensure safety and compliance with
32 flammability standards, the use of flame retardants (FRs) in various polymeric products is essential. Among all
33 kinds of FRs, brominated flame retardants (BFRs) are the most effective because they require the lowest amount
34 for the highest flame retardancy, thus their global market demand continues to increase substantially ([Birnbaum](#)
35 [and Staskal, 2004](#); [Bergman et al., 2012](#); [Gramatica et al., 2016](#)). At present, the market is witnessing a gradual
36 shift in demand for novel BFRs, in part driven by the phasing-out of widely used BFRs such as polybrominated
37 diphenyl ethers, now regulated by Stockholm Convention due to concerns over risks to public and ecosystem
38 health ([Bramwell et al., 2017](#); [Stubbings et al., 2019](#)). Apart from more than seventy-five kinds of conventional
39 BFRs, around sixty kinds of novel BFRs were reported to be used world-wide but also be ubiquitous in the
40 environment ([Georlette, 2001](#); [Liu et al., 2016](#); [Yu et al., 2016](#); [Zuiderveen et al., 2020](#)). Detailed reviews on
41 various BFRs have already been reported ([Alaee, 2003](#); [Covaci et al., 2011](#); [Ma et al., 2016](#)).

42 However, the presence of bromine in BFRs leads to many challenges whether on health and safety, due to
43 their toxicity, or on their proper disposal or recycling. Indeed, the occurrence of most BFRs in various
44 environmental matrices can cause adverse effects on diverse organisms through different modes of action, such
45 as hormone disruption and genotoxicity (Kim et al., 2014; Xiong et al., 2019). Incineration has the disadvantage
46 of generating corrosive or gases and possibly highly toxic dioxins (Sakai et al., 2001; Ni et al., 2012).
47 Landfilling results in the leaching of toxic brominated substance with the possible transfer into local aquifers,
48 especially in the case of additive BFRs that are simply blended with polymers (Zhou et al., 2013; Cristale et al.,
49 2019). Even in mechanically recycled plastics, uncontrolled BFR additives can cause fluctuation in their quality.
50 Therefore, the removal of BFRs from polymers has been a necessity in order to recycle or even simply dispose
51 them.

52 Solvent-based extraction has been proposed to remove BFRs from polymeric substrates with organic
53 solvents, such as toluene, methanol, or glycol ether based compounds (Nakajima et al., 2002; Altwaiq et al.,
54 2003; Zhang and Zhang, 2012). From the extractions, resulting polymers could be decontaminated and retained
55 most of their original qualities. Furthermore, solvents could be reused by distillation. Hence, some commercial
56 processes have been reported, like CreaSolv, which uses a combination of solvents to extract various BFRs
57 (Freegard et al., 2006). Although the process is effective, the use of organic solvents should be minimized due to
58 the related health and safety issues (toxicity, flammability, risks associated with distillation). Another drawback
59 of the traditional solvent extraction is that the subsequent distillation and drying processes are energy-intensive,
60 leading to increase in operational costs.

61 Supercritical CO₂ (ScCO₂) presents an attractive advantage over organic solvent for the extraction of
62 BFRs, mainly because it is cheap, non-toxic and non-flammable by nature, has high mass and thermal
63 diffusivity, and allows for an easy recovery by simple decompression of solvent-free extracted substances

64 (Taylor, 1996; Beckman, 2004). Solubility or saturated concentration is one of the most important parameters to
65 determine limits of extractability, thus, solubilities of some conventional BFRs have been measured in ScCO₂ as
66 function of pressure and temperature (Gamse et al., 2000; Peng et al., 2014). Also, ScCO₂ extraction of BFRs
67 was proved to be of various degrees of success in extraction efficiency with or without co-solvents, although the
68 solvation power of ScCO₂ is generally limited towards polar or high molecular weight compounds (Marioth et
69 al., 1996; Suzuki et al., 2002; Altwaiq et al., 2003). Otherwise, extraction kinetics must be investigated to
70 validate process scale-up and develop successful industrial processes (Nimet et al., 2011; Sodeifian et al., 2016;
71 Villanueva-Bermejo et al., 2020). Despite this, to our knowledge, there have only been few such studies reported
72 previously, either off-line or on-line, for BFR extraction (Bunte et al., 1996; Wang et al., 2004). This study
73 proposes to evaluate feasibility of BFR extraction using ScCO₂ considering thermodynamic and kinetic point of
74 view. We therefore report here a method coupling versatile high pressure vessel with both on-line UV-vis and
75 mid-IR spectrometers and demonstrate their applicability: (i) to perform spectroscopic analysis of multi-
76 component mixtures such binary and ternary mixtures in ScCO₂ media; and (ii) to investigate effects of
77 temperature, pressure, stirring, and matrix size on extraction kinetics for five BFRs, including three of the most
78 used conventional ones and two popular novel ones.

79 **2. Materials and methods**

80 *2.1 Materials*

81 Five selected BFR compounds: (i) 3,3',5,5'-Tetrabromobisphenol A (TBBPA) and (ii) 1,2,5,6,9,10-
82 Hexabromocyclododecane (HBCD) were purchased from Sigma-Aldrich (St. Louis, MO, USA); (iii)
83 Decabromodiphenyl ether (DBDBE) and (iv) 2,4,6-Tris(2,4,6-tribromophenoxy)-1,3,5-triazine (TTBP-TAZ)
84 were purchased from Macklin (Shanghai, China); (v) 2,2-Bis[3,5-dibromo-4-(2,3-

85 dibromopropoxy)phenyl]propane (TBBPA-BDBPE) was purchased from Aladdin (Shanghai, China). The BFRs'
86 Chemical structures and other detailed information are presented in Fig. S. 1 and table S. 1, respectively. Since
87 HBCD and DBDBE have relative lower purities, they were purified in flowing ScCO₂ at 60 °C and 25 MPa for 6 h
88 (Gamse et al., 2000). The other BFR compounds were used without any further purification.

89 Ultra-pure water was obtained from a water purification system (WaterPro[®], Labconco Co., USA), with a
90 resistivity of 18.2 MΩ·cm at 25 °C.

91 Liquid CO₂ was supplied by CryoExpress Pte. Ltd. (Singapore) with a purity of 99.9%.

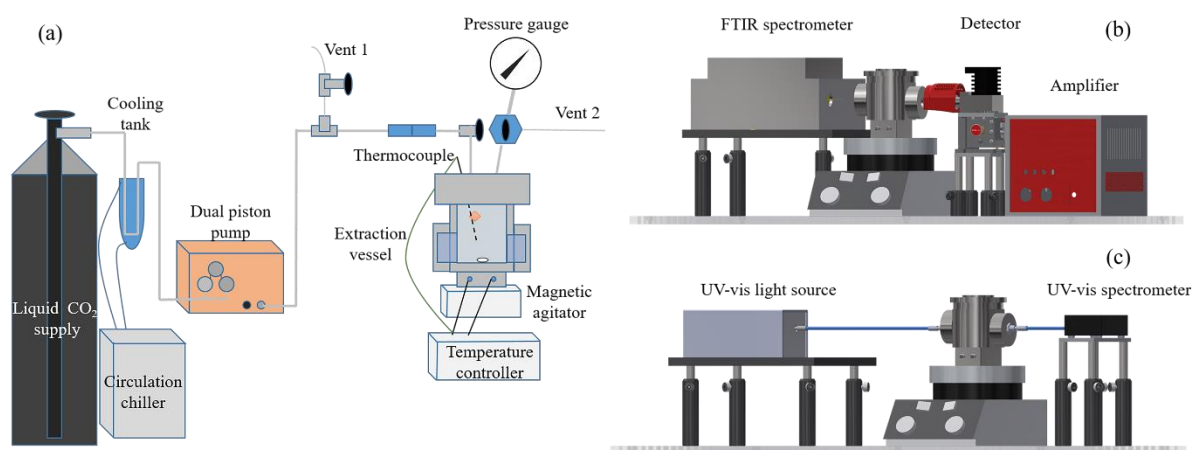
92 Acrylonitrile butadiene styrene (ABS) resin was selected as typical polymer substrate for additive BFRs
93 because it is commonly used in consumer products, such as housing of electric appliances, electronics, and toys.
94 BFR-free ABS and BFR-containing ABS pellets were fabricated as industrial practices by Shandong Tianyi
95 Chemical Co., Ltd. (China) as follows. Industrial grade TBBPA and TBBPA-BDBPE were respectively
96 incorporated in the BFR-free ABS resin by hot blending with a proportion of 13 wt.% and the resulted mixtures
97 were extruded to obtain pellets. We then grinded these as-purchased pellets into powders with a centrifugal mill
98 (ZM 200, Retsch, Germany), at cryogenic temperature using liquid N₂, then sieved the powders into two particle
99 size fractions (D_{ABS}) in the ranges: (i) 0.25-1 mm, and (ii) less than 0.25 mm.

100 2.2 Experimental apparatus

101 A schematic representation of our ScCO₂ extraction system optically coupled with on-line spectrometers
102 (FTIR and UV-vis) is shown in Fig. 1. The core part of the system, the extraction reactor, is a commercial
103 pressure vessel from Parr Instrumental Company, USA (ref. 2430HC2), modified as per our requirements with
104 optical windows to enable spectroscopic studies for operating pressure and temperature ranging up to 35 MPa
105 and 200 °C. The vessel has an entire volume of 75.4 mL, with minimized dead volumes from filling and venting
106 ports. Two dismountable windows (made of sapphire for FTIR or fused silica for UV-vis; rupture modulus: 1200

107 MPa versus 100 MPa; diameter: 25 mm; thickness: 15.7 mm) are located on each side of the vessel in
 108 opposition to each other. Each window is maintained in place thanks to a window holder and sealed by a Teflon
 109 O-ring and a Teflon cushion through “opposed force” (Fig. S. 2). The resulted optical path length is measured of
 110 58 mm, sufficiently long to give desired sensitivity and limits of detectability (Jackson et al., 1995; Poliakoff et
 111 al., 1995).

112 For the other parts of the ScCO₂ extraction system (Fig. 1a), liquid CO₂ coming from a liquid tank is first
 113 cooled by a circulation chiller (F250, Julabo, Germany) prior to its delivery to a pressure dual piston pump (LD-
 114 Class, Teledyne ISCO, USA). The vessel temperature is monitored using a K-type thermocouple inserted into a
 115 stainless steel plunger. Two PID controlled (E5CC, Omron, Japan) electric cartridge heaters, slid into cavities in
 116 the bottom of the vessel, are used to raise the vessel’s temperature. A magnetic agitator (MR 3001 K, Heidolph,
 117 Germany) drives a 12 × 3 mm Teflon-coated stirring bar to stir the contents in the vessel. Additional accessories
 118 permit measurements of pressure, temperature, and agitation speed with a precision of 0.1 MPa, 0.1°C, and 3%,
 119 respectively.



120
 121 **Fig. 1.** Schematic illustration of the experimental ScCO₂ extraction system (a), where each component of the system is not
 122 presented in proportion; the virtual deployment of the vessel with FTIR (b) and with UV-vis spectroscopic components (c),
 123 and the vessel head parts (model 4792) and the spilt rings (A455HC) are abridged for clearly presenting their optical

124 alignment.

125 The spectroscopic components are combined with the ScCO₂ extraction system in a modular fashion (Fig.
126 1b and Fig. 1c). Their optical alignment is readily adjusted thanks to bases and supporting rods purchased from
127 Thorlabs Inc. (USA). The IR beam provided by a FTIR spectrometer (Bruker Alpha OEM, Bruker Optics Inc.,
128 Germany) transmits through the vessel, and the signal are detected by a Stirling Cycle Cooled detector
129 connected with an amplifier (K508-MCT1000, Infrared Associates, U.S.A). They were initially integrated as an
130 on-line monitoring of microfluidic processes (C. Penisson, 2018; Kokoric et al., 2018; Maurice et al., 2020) and
131 have been reconverted here for the purpose of its extraction reactor.

132 For UV-vis monitoring, the UV radiation emanating from a deuterium light source (DH-MINI, Ocean
133 Optics Inc., UK) transfers through the vessel, a pair of optical fibers, and several collimating lens. Spectra were
134 recorded by a UV-vis spectrometer (Flame-T, Ocean Optics Inc., UK).

135 *2.3 Measurement of extraction kinetics*

136 All BFR extraction experiments in ScCO₂ were carried out using a solid-supercritical fluid extraction
137 process. Prior to each extraction, a thorough clean-up of the ScCO₂ extraction system was performed with
138 flowing ScCO₂ until no extra absorbance of contents was detected, and then reference spectra of pure ScCO₂
139 were taken using identical operating conditions as sample spectra. To assess reproducibility and improve
140 precision, each extraction was performed in triplicate. Precisely weighted pure BFR powders (100 mg) or ABS
141 powders (600 mg) were enclosed within Solidweave mesh (Mesh size=9 μm) folded uniformly like a mailing
142 envelope, which was then attached inside the vessel at the top of the thermocouple inverted finger, close to the
143 filling port. After loading the sample, the vessel was hermetically closed and then flushed three times with
144 gaseous CO₂. Then it typically took around 10 minutes to heat it and fill it in with compressed CO₂ to the
145 desired temperature and pressure, prior to stirring at a set speed. Spectra were collected at regular intervals

146 during the whole extraction process. IR spectra were collected with a 4 cm^{-1} resolution and were obtained by the
147 Fourier transformation of 64 interferograms. UV spectra were averaged from 1000 scans within an integration
148 time of 0.015 s. Each extraction experiment was terminated after reaching a steady state where spectra no longer
149 show any change in absorbance. The decompression procedure was fast (less than 10 s) along with subsequent
150 refilling with gaseous CO_2 and no re-deposition of solute back to sample mesh could be observed under a
151 microscope ($\times 500$, RS Pro).

152 *2.4 Determination of saturated concentration*

153 Saturated concentration (c_s , in mmol/L) is the maximum concentration of a solute dissolved in a solvent. c_s
154 of individual pure BFR in ScCO_2 was measured gravimetrically using an analytical balance (MS105, Mettler-
155 Toledo, USA) with a readability of 0.01 mg and was calculated with the following equation:

$$156 \quad c_s = 10^3 \cdot (m_2 - m_1) / [M_{\text{BFR}} \cdot (V_v - V_s)] \quad (1)$$

157 where m_1 and m_2 indicate the weight of sample package before and after extraction; M_{BFR} denotes the molar
158 mass of the used BFR molecule. V_v is the vessel volume (75.4 mL) and V_s is the sample package volume
159 determined with the water discharging method.

160 Since mass removal of BFR is not measurable gravimetrically for ABS samples, Br content changes of
161 ABS samples before and after extraction were determined with an X-ray fluorescence analyzer (XRF) (Vanta C,
162 Olympus, Japan) applying RoHS plus method. For this determination, the powdered ABS samples (200 mg)
163 were pressed into a circular shaped disc using a hydraulic crimper (MSK-510M, MTI Co., China) at $160\text{ }^\circ\text{C}$ and
164 5 MPa for 5 min. The mass removal of BFR can be calculated by dividing Br content of BFR from Br content
165 difference of the ABS sample, thus the saturated concentration can be calculated with Eq. (1) as well.

166 All experimental data was displayed in a format of mean value \pm standard deviation.

167 *2.5 IR spectroscopy and data processing*

168 The IR spectra were processed with a software combination of OPUS 7.5 and Python 3.6.8. After baseline
169 correction, the corresponding absorbance peak of interest (A) (Table S. 2) was integrated in the wavenumber
170 region of w_2-w_1 (in cm^{-1}) using the following equation:

$$171 \quad A = \int_{w_1}^{w_2} \log_{10} \left(\frac{I_0}{I_t} \right) dw \quad (2)$$

172 with I_0 and I as sample and baseline intensity, respectively.

173 According to Beer-Lambert Law, the integrated absorbance was proportionally converted to BFR
174 concentration (c , in mmol/L) in ScCO_2 (IUPAC, 1997):

$$175 \quad c_t = A_t \cdot c_s / A_s \quad (3)$$

176 where the subscripts t and s indicate timely and saturation readings.

177 Furthermore, the linear sum of the absorbance spectra of each component (A_i) was considered for
178 quantitative interpretation of the overlapped peak area of a mixture (A_m):

$$179 \quad A_m = \sum_{i=1}^N A_i \quad (4)$$

180 *2.6 Mathematical modelling of extraction kinetics*

181 In outline, the ScCO_2 extraction of compounds from solid matrices (porous or not) can be condensed into a
182 four-step process: (i) diffusion of ScCO_2 into internal structure of solid matrices; (ii) desorption and solvation of
183 solute in the ScCO_2 ; (iii) intra-particle diffusion of the mixture of solute and ScCO_2 to solid interface; and (iv)
184 diffusion of the mixture from the solid interface to bulk ScCO_2 (Madras et al., 1994; Sunarso and Ismadji, 2009;
185 Huang et al., 2012). All these steps are diffusion limiting steps except for the solubilization step (ii).

186 To achieve specific description of extraction kinetics involving complex phenomena with mathematical
187 models, we introduced two simplified scenarios, including absence of matrix and well stirred reactor, based on
188 the assumption that the diffusion steps can be controlled by changing of matrix properties or stirring speed, and

189 hence basic physicochemical models could be applied (Srinivasan et al., 1990). For the solubilization step, an
 190 irreversible and first order model (linear desorption) was applied to calculate solubilization rate coefficient (k_s , in
 191 h^{-1}) over extraction period (t , in h) with the following equation (Tan and Liou, 1989; Elektorowicz et al., 2007;
 192 Jokić et al., 2010):

$$193 \quad \frac{dc}{dt} = k_s(c_s - c_t) \quad (5)$$

194 and with the initial condition:

$$195 \quad t = 0 \text{ h}, c_t = 0 \text{ mmol/L} \quad (6)$$

196 After solving by integration on both sides of the Eq. (5), one can get

$$197 \quad \ln[(c_s - c_t)/c_s] = -k_s \cdot t \quad (7)$$

198 The applied model for the diffusion steps is based on the hot sphere diffusion model derived from Fick's diffusion
 199 laws assuming that loaded particles consist of solid spheres with uniform radius and initial concentration of
 200 extracted substance and are immersed into a fluid free from the substance (Crank, 1979; Bartle et al., 1990; Huang
 201 et al., 2012). The model is expressed as:

$$202 \quad \frac{c_t}{c_s} = 1 - \frac{6}{\pi^2} \sum_{n=1}^{\infty} \frac{1}{n^2} \cdot \exp \left[- \left(\frac{n\pi}{R} \right)^2 D_e t \right] \quad (8)$$

203 with D_e as effective diffusion coefficient in a solid substrate (m^2/h) and R as radius of spherical solid particles
 204 (m).

205 For long time, all terms except the first in the series of exponential terms in Eq. (8) become negligible and the
 206 kinetic curve can be rewritten as:

$$207 \quad \ln[(c_s - c_t)/c_s] = \ln \left(\frac{6}{\pi^2} \right) - \frac{\pi^2 D_e}{R^2} \cdot t \quad (9)$$

208 where $\pi^2 D_e / R^2$ may also be recast as diffusion rate coefficient k_D (h^{-1}).

209 From Eq. (7) and Eq. (9), a plot of $\ln[(c_s - c_t)/c_s]$ versus t may fall onto two intersecting straight lines with
 210 different slopes k_1 and k_2 (Subra et al., 1998; Hojnik et al., 2008).

211 In addition, absolute average relative deviations (*AARD*, %) between experimental data ($c_{t,\text{exp}}$) and modeled data
212 ($c_{t,\text{mod}}$) are also evaluated by:

$$213 \quad AARD = \frac{100}{N} \sum_{i=1}^N \frac{|c_{t,\text{exp}} - c_{t,\text{mod}}|}{c_{t,\text{exp}}} \quad (10)$$

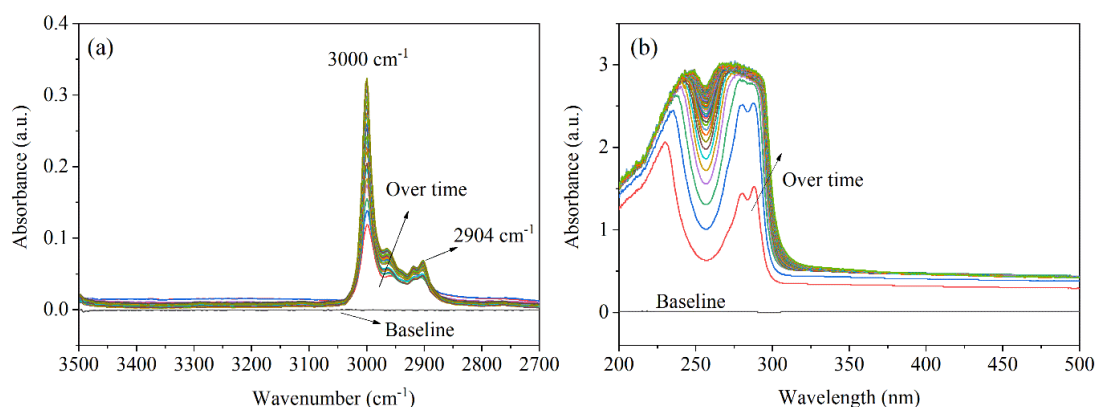
214 3. Results and discussion

215 3.1 Comparison between FTIR and UV-vis spectroscopies

216 Spectroscopic monitoring, including vibrational and electronic spectroscopies, is a classical on-line
217 technique in many supercritical process studies because it allows for rapid and inexpensive determination of
218 concentration with relatively small amounts of compound (Laintz et al., 1991; Carrott and Wai, 1998; Wang et
219 al., 2004; Wang et al., 2018). In this study, FTIR and UV-vis spectroscopies were first compared for their
220 applicability to characterize BFR compounds in ScCO₂. Raman spectroscopy was not considered since it suffers
221 from a lack of sensitivity when solute concentrations are low (Jackson et al., 1995). In terms of spectrum
222 window, the FTIR reference spectrum was narrowed to two available bands of 4500-3880 cm⁻¹ and of 3500-
223 2600 cm⁻¹ (Fig. S. 3a). The other IR bands, including the characteristic C-Br group (690-515 cm⁻¹), were
224 completely obscured by absorptions of sapphire windows and ScCO₂, itself (Poliakoff et al., 1995). To
225 circumvent this problem, some identifiable groups, like ν (C-H) and ν (O-H), were employed to characterize
226 BFRs in ScCO₂ (Table S. 2). However, due to the ubiquity of these groups in organic chemicals, the high purity
227 of BFR compounds and the cleanliness of reference spectra are essential to characterize BFRs in ScCO₂,
228 especially for a quantitative purpose. Comparatively, the spectrum window of UV-vis could extend to almost the
229 whole spectrometer's range (200-800 nm) (Fig. S. 3b).

230 With well-defined reference spectra, TBBPA, the most commercially used BFR, was characterized as an
231 example in ScCO₂ using FTIR and UV-vis spectrometers, respectively (Fig. 2). Both spectra demonstrated

232 incremental absorbance over extraction time until they leveled off and reached a stable value. The FTIR
233 spectrum of TBBPA was marked by two bands, with two maximum absorbance located at 2904 cm^{-1} and 3000
234 cm^{-1} , resulting from ν (C-H alkane) and composite ν (C-H combinations) absorption, respectively (Fulton et al.,
235 1993). In the UV-vis spectrum, TBBPA showed two absorption band (200-260 nm and 260-310 nm) as a result
236 of electronic transitions, $\pi \rightarrow \pi^*$ transition (conjugated C=C group), which was similar to the spectrum of
237 TBBPA through organic solvent presented previously (Lu et al., 1999; Khaled et al., 2018). However, the UV-
238 vis spectrum of TBBPA exposed an absorbance saturation problem. The high absorptivity of the chromophore in
239 the UV region set an upper limit of detection, although the issue can be modified by replacing thicker windows
240 to shorten the optical path length. Besides, a shift of peaks in the UV-vis spectrum was apparent with the
241 increase of concentration, which resulted in the ambiguous peaks' interpretation.

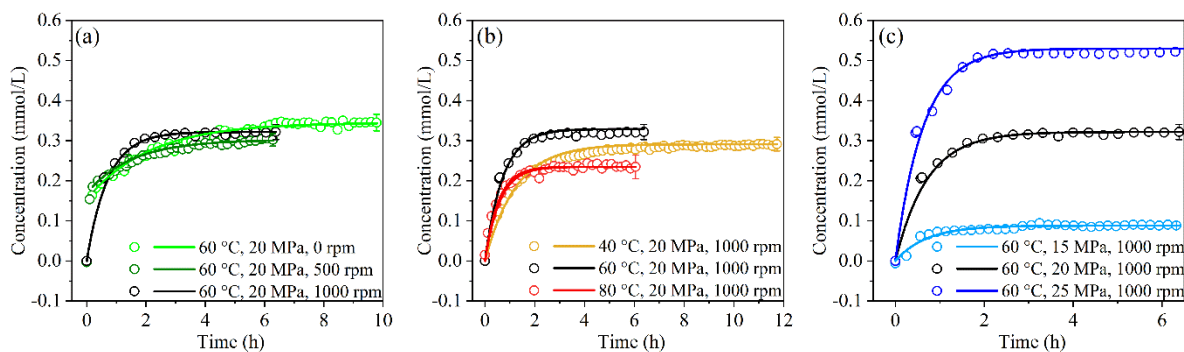


242
243 **Fig. 2** FTIR (a) and UV-vis (b) spectra of TBBPA in ScCO₂ over extraction period at 60°C, 20 MPa, and 1000 rpm.

244 Although each of the technique has its own advantages and shortcomings from the spectroscopic
245 standpoint, FTIR is a better technique than UV-Vis for carrying out the on-line monitoring. In addition, the
246 higher rupture modulus of sapphire than fused silica will facilitate a safer operating condition under high
247 pressure. Therefore, only FTIR spectroscopy was used in the following sections.

248 3.2 Effect of operating conditions

249 To study the influence of operating conditions on extraction performance of BFR in ScCO_2 , BFR+ ScCO_2
 250 binary system was first explored based on a simplified scenario in which the matrix was absent and matrix
 251 related diffusion steps (i) and (iii) might be negligible (see section 2.6). Regarding the binary equilibria of
 252 TBBPA and ScCO_2 , the list of operating conditions explored and the fitting parameters are given in Table 1 and
 253 corresponding kinetic curves are illustrated in Fig. 3. The good agreement of c_s result of TBBPA at 60 °C, 20
 254 MPa and 0 rpm with published one (Gamse et al., 2000) allowed to validate our apparatus for c_s measurement.
 255 Additionally, all the kinetic curves showed similar trend that the concentration approached its asymptotic value
 256 gradually after an initial rapid extraction period.



257
 258 **Fig. 3** Influence of operating conditions on ScCO_2 extraction kinetics of TBBPA: stirring speed (a), temperature (b), and
 259 pressure (c), discrete points and lines denote *experimental* and fitted results, respectively.

Table 1 Saturated concentration and kinetic parameters of selected BFRs in binary system.

BFRs	Operating conditions	c_s	k_s	AARD
		mmol/L	h ⁻¹	%
TBBPA	40 °C, 20 MPa, 1000 rpm	0.291±0.004	0.81±0.04	3.16
	60 °C, 15 MPa, 1000 rpm	0.088±0.004	1.43±0.19	4.14
	60 °C, 20 MPa, 0 rpm	0.345±0.021	0.48±0.03	2.52
	60 °C, 20 MPa, 500 rpm	0.302±0.016	0.66±0.04	2.28
	60 °C, 20 MPa, 1000 rpm	0.322±0.019	1.40±0.04	1.11
	60 °C, 25 MPa, 1000 rpm	0.531±0.014	1.59±0.08	2.22
	80 °C, 20 MPa, 1000 rpm	0.235±0.007	1.84±0.09	3.70
HBCD	60 °C, 25 MPa, 1000 rpm	0.064±0.004	4.68±1.09	4.22
DBDPE	60 °C, 25 MPa, 1000 rpm	0.004±0.000	N.C.	N.C.
TBBPA-BDBPE	60 °C, 25 MPa, 1000 rpm	0.154±0.002	4.68±0.91	5.70
TTBP-TAZ	60 °C, 25 MPa, 1000 rpm	0.012±0.000	8.10±1.06	3.71

261 N.C. means not calculated.

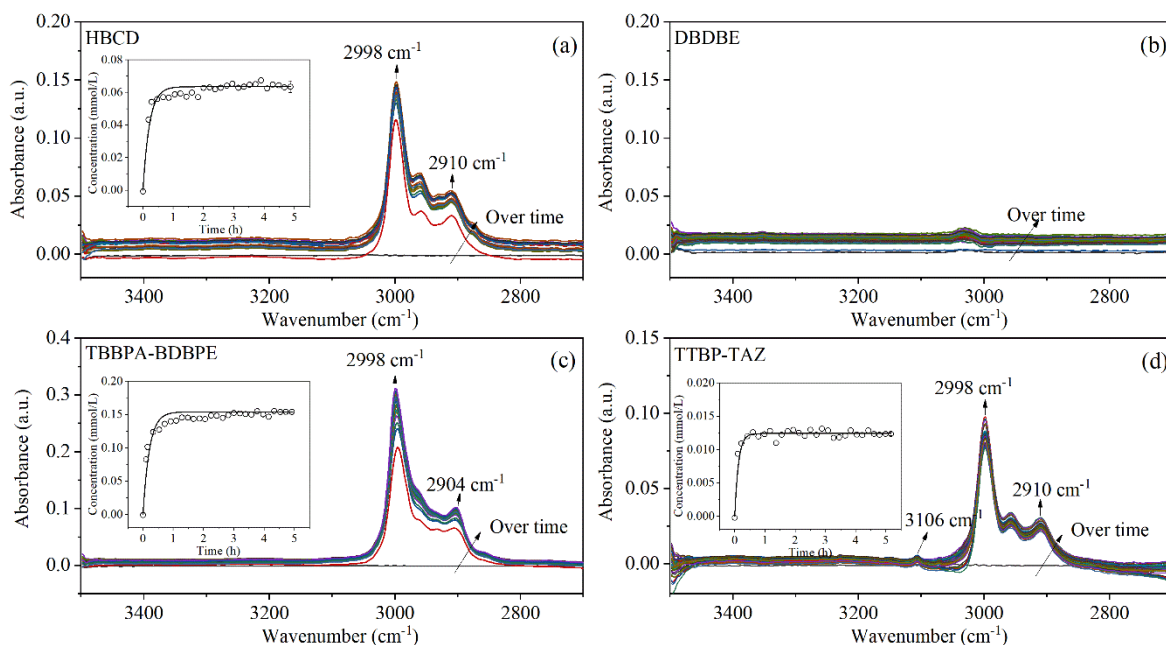
262 Stirring was found to improve the extraction kinetic and shorten the time required to achieve saturation
 263 from 6 hours down to 2 hours, when comparing the three cases of non-stirring, 500 rpm, and 1000 rpm (Fig. 3a).
 264 Only at the highest stirring speed could the overall experimental scatterplots be fitted well with a first order
 265 kinetic equation (Eq. 5), indicating the external diffusion step is negligible in the well stirred reactor (the second
 266 simplified scenario, see section 2.6) by fast stirring and leading to a solubilization-dominated process. Whereas,
 267 external diffusion becomes more significant with less powerful stirring. Since the rapid increase of
 268 concentration during the initial compression period was owing to the inevitable agitation caused by filling

269 turbulences, the fitting model was applied after the initial compression period in the 0 rpm and 500 rpm cases,
270 where the decreased k_s can only be attributed to external diffusion. Besides, stirring had insignificant impact on
271 the solubility of TBBPA considering the measurement's uncertainties of the experiments.

272 The effects of temperature and pressure on extraction of TBBPA were explored at a constant stirring speed
273 of 1000 rpm (Fig. 3b and Fig. 3c). The k_s value more than doubled with the increase of temperature from 40 °C
274 to 80 °C, while the highest c_s occurred at the intermediate temperature of 60 °C for the studied pressure.
275 Furthermore, temperature dependent rate coefficients accorded well with Arrhenius equation which states that
276 the natural logarithm of rate coefficient is proportional to the inverse of absolute temperature (Connors, 1990).
277 However, we observed that the k_s value was barely influenced by pressure increased from 15 to 25 MPa at
278 60 °C, although the solubility was significantly improved. Previous reports have concluded that high
279 extractability of BFRs in ScCO₂ is generally achieved at high temperature and pressure (Gamse et al., 2000;
280 Suzuki et al., 2002).

281 Given consideration of both kinetic and thermodynamic aspects, an optimized operating condition (60 °C,
282 25 MPa, 1000 rpm) was also applied for the other four BFRs. As shown in Fig. 4, each BFR had a fingerprint
283 spectrum within the band of 3800-2700 cm⁻¹, resulting in a kinetic curve except for DBDBE, which does not
284 contain any identifiable groups in its chemical structure. The specific spectral patterns were also verified by
285 additional ATR-FTIR characterizations of pure BFR powders (Fig. S. 4). Actually, compared with ATR-FTIR
286 spectra, the on-line FTIR spectra showed slight difference in a red shift phenomenon due to the formation of
287 hydrogen bonding in ScCO₂ and in relative absorbance intensity of different groups due to the existence of
288 ScCO₂ and sapphire windows (Fulton et al., 1993; Poliakoff et al., 1995). Regarding to the extraction
289 performances of HBCD, TBBPA-BDBPE, and TTBP-TAZ in ScCO₂, saturated concentrations were lower but
290 periods required to reach equilibria were all below one hour with comparison to TBBPA. DBDBE had the

291 lowest solubility, hence it was identified as the most difficult BFR to extract (Peng et al., 2014). Overall, high
 292 rate coefficients indicate that a dynamic extraction with fast flowing ScCO₂ could be an efficient process,
 293 because concentration gradient can be kept high enough to drive the extraction in a stationary mode.



294
 295 Fig. 4 FTIR spectra over extraction period and resulted kinetic curves of four BFRs at 60 °C, 25 MPa, and 1000 rpm.

296 3.3 Effect of loading water as cosolvent

297 In ternary systems, water was first included as cosolvent along with BFR and ScCO₂ since a small amount
 298 of water added to ScCO₂ was reported to increase the solubility of polar species in nonpolar solvent (Jackson et
 299 al., 1995). Other organic solvents were not included because of their high miscibility in ScCO₂ inducing a large
 300 IR absorbance in the studied band. The FTIR spectra of TBBPA with loading of ultra-pure water (200 μL, below
 301 saturation) were recorded over the extraction period (Fig. S. 5a). The absorbance caused by O-H stretching of
 302 H₂O molecules did not interfere with the absorbance of TBBPA, thus kinetic curve for both TBBPA and H₂O
 303 can be followed simultaneously (Fig. S. 5b). Water was faster to reach equilibrium than TBBPA. Despite an
 304 improved *c_s* of TBBPA by 7% in the presence of such small amount of water, its *k_S* decreased by 43% probably

305 due to competitive association between TBBPA and H₂O molecules with ScCO₂ (Table 1 and Table 2). Thus, an
 306 optimum of extraction performance in the presence of water has to be included in future research. Herein, FTIR
 307 spectroscopy provides another advantage over UV-vis spectroscopy because water lack spectral transitions in
 308 the UV region.

309 Table 2 Saturated concentration and kinetic parameters of selected BFRs in ternary systems at 60 °C, 25 MPa, 1000 rpm

BFRs	Cosolvent or matrix effect	c_s	k_s	k_D	D_e	AARD
		mmol/L	h ⁻¹	h ⁻¹	m ² /h	%
BFR+H₂O+ScCO₂						
TBBPA	Loading of 200 μL H ₂ O	0.570±0.007	0.91±0.05	N.C.	N.C.	3.59
BFR/ABS+ScCO₂						
TBBPA	$D_{ABS} < 0.25$ mm	0.333±0.001	1.78±0.08	1.08±0.05	$< 1.7 \times 10^{-9}$	2.04
TBBPA	$D_{ABS} 0.25-1$ mm	0.331±0.001	0.49±0.08	0.25±0.02	$4.0 \times 10^{-10}-6.3 \times 10^{-9}$	1.95
TBBPA-BDBPE	$D_{ABS} < 0.25$ mm	0.219±0.004	1.94±0.37	1.32±0.08	$< 2.1 \times 10^{-9}$	2.88

310 N.C. means not calculated.

311 3.4 Effect of ABS matrix

312 To discover the matrix effect on extraction performance, BFR-free ABS resin was used as polymeric
 313 substrate to incorporate with BFRs, including TBBPA and TBBPA-BDBPE. The FTIR spectra of each extraction
 314 experiment are presented in Fig. S. 6. The extraction of ABS resin itself can also be observed, indicating that
 315 ScCO₂ has a certain solvation power on ABS, which can increase with temperature and pressure, leading to
 316 undesired dissolution of polymers or oligomers into ScCO₂ (Sikorski, 1993; Zhao et al., 2018). In the case of
 317 TBBPA-incorporated samples, the effect of particle size was investigated on their extraction performance, as
 318 shown in Fig. S. 7. Obviously, the finer particle size, the faster the extraction process. The kinetic curve can be

319 decomposed in two phases, with a first rapid extraction followed by a slower one. Their c_s of TBBPA were of
320 similar value, 0.33 mmol/L, lower than that of extraction without ABS matrix (0.53 mmol/L) due to the
321 competitive dissolution of ABS polymers.

322 According to the broken and intact cell concept, analytes can be distributed at the outer surface of particles
323 and embedded into their inner structure, just as BFR-incorporated ABS powders after grinding, resulting in
324 easily accessible BFRs and less accessible BFRs, respectively (Sovová, 1994). Hence, the first rapid extraction
325 of so-called washing process was controlled by solubilization in the well stirred reactor and k_1 can be assigned to
326 k_s (Table 2). Furthermore, the sudden reduction of extraction rate after the first part indicates the completion of
327 accessible BFR's extraction and the intra-particle diffusion resistance came into the effect (Srinivasan et al.,
328 1990; Alexandrou et al., 1992; Grosso et al., 2010). Hereby, k_D can be calculated by $k_D = k_1 - k_2$ and D_e range can
329 also be estimated according to Eq. (9). The TBBPA-BDBPE incorporated samples also supported the two-stage
330 extraction process and the applied models provided very good approximation of experimental data with *AARD*
331 lower than 2.9%.

332 4. Conclusions

333 In this study, a supercritical reactor was assembled with on-line spectroscopic components to study ScCO₂
334 extraction of BFRs. A notable feature of the apparatus, applicable beyond the current study, is the compatibility
335 with both UV-vis and FTIR spectrometer using the same vessel, enabling to acquire more abundant spectral
336 information of multi-component mixtures in real time and follow their kinetics. For quantitatively characterizing
337 BFRs in ScCO₂, FTIR spectroscopy is preferable to UV-vis due to its proper detection range and clearer spectral
338 interpretation despite its limited spectra window. Five BFR molecules were studied using the on-line FTIR
339 technique along with mathematical modelling. Stirring speed, temperature, and particle size were found to

340 significantly influence extraction kinetics while pressure did not in the considered range. Sufficiently fast
341 stirring could eliminate limitations due to diffusion of molecules in ScCO₂, and both higher temperature and
342 finer grinding size accelerate extraction kinetic. Therefore, high extraction rates could compensate for low
343 solubility if one applies a dynamic extraction with flowing ScCO₂. Furthermore, extraction parameters provided
344 here are valuable to enable a scale-up process design.

345

346 **CRedit authorship contribution statement**

347 **Dong Xia:** Methodology, Investigation, Formal analysis, Writing - original draft. **Ange Maurice:** Software.

348 **Antoine Leybros:** Methodology, Writing - review & editing. **Jong-Min Lee:** Funding acquisition, Resources.

349 **Agnes Grandjean:** Funding acquisition, Formal analysis, Writing - Review & Editing. **Jean-Christophe P.**

350 **Gabriel:** Funding acquisition, Resources, Conceptualization, Methodology, Writing - review & editing,

351 Supervision, Project administration.

352

353 **Acknowledgments**

354 We acknowledge intern Li-Yi Ang for her assistance in experimental investigation during her Final Year Project

355 in Nanyang Technological University. JCG acknowledge the Region Pays de la Loire for “Young Researcher”

356 funding for the purchase of Parr ScCO₂ core reactor (1999). All authors acknowledge financial support from

357 SCARCE laboratory. SCARCE is supported by the National Research Foundation, Prime Minister’s Office,

358 Singapore, the Ministry of National Development, Singapore, and National Environment Agency, Ministry of

359 the Environment and Water Resource, Singapore under the Closing the Waste Loop R&D Initiative as part of the

360 Urban Solutions & Sustainability - Integration Fund (Award No. USS-IF-2018-4).

361 **Reference**

- 362 Alaei, M., 2003. An overview of commercially used brominated flame retardants, their applications, their use patterns in
363 different countries/regions and possible modes of release. *Environ. Int.* 29, 683-689. <https://doi.org/10.1016/S0160->
364 4120(03)00121-1.
- 365 Alexandrou, N., Lawrence, M.J., Pawliszyn, J., 1992. Cleanup of complex organic mixtures using supercritical fluids and
366 selective adsorbents. *Anal. Chem.* 64, 301-311. <https://doi.org/10.1021/ac00027a011>.
- 367 Altwaiq, A.m., Wolf, M., van Eldik, R., 2003. Extraction of brominated flame retardants from polymeric waste material using
368 different solvents and supercritical carbon dioxide. *Anal. Chim. Acta* 491, 111-123. <https://doi.org/10.1016/S0003->
369 2670(03)00785-2.
- 370 Bartle, K.D., Clifford, A.A., Hawthorne, S.B., Langenfeld, J.J., Miller, D.J., Robinson, R., 1990. A model for dynamic
371 extraction using a supercritical fluid. *J. Supercrit. Fluids* 3, 143-149. [https://doi.org/10.1016/0896-8446\(90\)90039-O](https://doi.org/10.1016/0896-8446(90)90039-O).
- 372 Beckman, E.J., 2004. Supercritical and near-critical CO₂ in green chemical synthesis and processing. *J. Supercrit. Fluids* 28,
373 121-191. [https://doi.org/10.1016/S0896-8446\(03\)00029-9](https://doi.org/10.1016/S0896-8446(03)00029-9).
- 374 Bergman, Å., Rydén, A., Law, R.J., de Boer, J., Covaci, A., Alaei, M., Birnbaum, L., Petreas, M., Rose, M., Sakai, S., 2012.
375 A novel abbreviation standard for organobromine, organochlorine and organophosphorus flame retardants and some
376 characteristics of the chemicals. *Environ. Int.* 49, 57-82. <https://doi.org/10.1016/j.envint.2012.08.003>.
- 377 Birnbaum, L.S., Staskal, D.F., 2004. Brominated flame retardants: cause for concern? *Environ. Health Perspect.* 112, 9-17.
378 <https://doi.org/10.1289/ehp.6559>.
- 379 Bramwell, L., Harrad, S., Abdallah, M.A.-E., Rauert, C., Rose, M., Fernandes, A., Pless-Mullooli, T., 2017. Predictors of human
380 PBDE body burdens for a UK cohort. *Chemosphere* 189, 186-197. <https://doi.org/10.1016/j.chemosphere.2017.08.062>.
- 381 Bunte, G., Haerdle, T., Krause, H., Marioth, E., 1996. Extraction of brominated flame retardents with supercritical CO₂.
382 *Process Technology Proceedings*. Elsevier, pp. 535-539. [https://doi.org/10.1016/S0921-8610\(96\)80093-8](https://doi.org/10.1016/S0921-8610(96)80093-8).

383 C. Penisson, A.W., J. Theisen, V. Kokoric, B. Mizaikoff, J.C.P. Gabriel, 2018. Water activity measurement of NaCl/H₂O
384 mixtures via substrate-integrated hollow waveguide infrared spectroscopy with integrated microfluidics. *Nanotech* 2018. CRC
385 Press, Anaheim, CA, USA, pp. 198-201.

386 Carrott, M., Wai, C., 1998. UV– visible spectroscopic measurement of solubilities in supercritical CO₂ using high-pressure
387 fiber-optic cells. *Anal. Chem.* 70, 2421-2425. <https://doi.org/10.1021/ac971077h>.

388 Connors, K.A., 1990. *Chemical kinetics: the study of reaction rates in solution*. Wiley-VCH Verlag GmbH.

389 Covaci, A., Harrad, S., Abdallah, M.A., Ali, N., Law, R.J., Herzke, D., de Wit, C.A., 2011. Novel brominated flame retardants:
390 a review of their analysis, environmental fate and behaviour. *Environ. Int.* 37, 532-556.
391 <https://doi.org/10.1016/j.envint.2010.11.007>.

392 Crank, J., 1979. *The mathematics of diffusion*. Oxford university press.

393 Cristale, J., Belé, T.G.A., Lacorte, S., de Marchi, M.R.R., 2019. Occurrence of flame retardants in landfills: A case study in
394 Brazil. *Environ. Res.* 168, 420-427. <https://doi.org/10.1016/j.envres.2018.10.010>.

395 Elektorowicz, M., El-Sadi, H., Lin, J., Ayadat, T., 2007. Effect of supercritical fluid extraction parameters and clay properties
396 on the efficiency of phenanthrene extraction. *J. Colloid Interface Sci.* 309, 445-452. <https://doi.org/10.1016/j.jcis.2006.12.038>.

397 Freegard, K., Tan, G., Morton, R., 2006. *Develop a Process to Separate Brominated Flame Retardants from WEEE Polymers–*
398 *Final report. Waste & Resources Action Programme (WRAP)*.

399 Fulton, J.L., Yee, G.G., Smith, R.D., 1993. *Hydrogen Bonding of Simple Alcohols in Supercritical Fluids: An FTIR Study*.
400 *Supercritical Fluid Engineering Science*. ACS Publications. <https://doi.org/10.1021/bk-1992-0514.ch014>.

401 Gamse, T., Steinkellner, F., Marr, R., Alessi, P., Kikic, I., 2000. Solubility studies of organic flame retardants in supercritical
402 CO₂. *Ind. Eng. Chem. Res.* 39, 4888-4890. <https://doi.org/10.1021/ie000231e>.

403 Georlette, P., 2001. New brominated flame retardants meet requirements for technical plastics. *Plastics, Additives and*
404 *Compounding* 3, 28-33. [https://doi.org/10.1016/S1464-391X\(01\)80134-3](https://doi.org/10.1016/S1464-391X(01)80134-3).

405 Gramatica, P., Cassani, S., Sangion, A., 2016. Are some “safer alternatives” hazardous as PBTs? The case study of new flame
406 retardants. *J. Hazard. Mater.* 306, 237-246. <https://doi.org/10.1016/j.jhazmat.2015.12.017>.

407 Grosso, C., Coelho, J., Pessoa, F., Fareleira, J., Barroso, J., Urieta, J., Palavra, A., Sovova, H., 2010. Mathematical modelling
408 of supercritical CO₂ extraction of volatile oils from aromatic plants. *Chem. Eng. Sci.* 65, 3579-3590.
409 <https://doi.org/10.1016/j.ces.2010.02.046>.

410 Hojnik, M., Škerget, M., Knez, Ž., 2008. Extraction of lutein from Marigold flower petals—Experimental kinetics and
411 modelling. *LWT-Food Sci. Technol.* 41. <https://doi.org/10.1016/j.lwt.2007.11.017>.

412 Huang, Z., Shi, X.-h., Jiang, W.-j., 2012. Theoretical models for supercritical fluid extraction. *J. Chromatogr. A* 1250, 2-26.
413 <https://doi.org/10.1016/j.chroma.2012.04.032>.

414 IUPAC, 1997. *Compendium of chemical terminology*. Blackwell Scientific Publications Oxford.
415 <https://doi.org/10.1351/goldbook.B00626>.

416 Jackson, K., Bowman, L.E., Fulton, J.L., 1995. Water solubility measurements in supercritical fluids and high-pressure liquids
417 using near-infrared spectroscopy. *Anal. Chem.* 67, 2368-2372. <https://doi.org/10.1021/ac00110a007>.

418 Jokić, S., Velić, D., Bilić, M., Bučić-koJić, A., PIANiNić, M., ToMAS, S., 2010. Modelling of solid-liquid extraction process
419 of total polyphenols from soybeans. *Czech Journal of Food Sciences* 28, 206-212. <https://doi.org/10.17221/200/2009-CJFS>.

420 Khaled, A., Richard, C., Rivaton, A., Jaber, F., Sleiman, M., 2018. Photodegradation of brominated flame retardants in
421 polystyrene: Quantum yields, products and influencing factors. *Chemosphere* 211, 943-951.
422 <https://doi.org/10.1016/j.chemosphere.2018.07.147>.

423 Kim, Y.R., Harden, F.A., Toms, L.-M.L., Norman, R.E., 2014. Health consequences of exposure to brominated flame retardants:
424 a systematic review. *Chemosphere* 106, 1-19. <https://doi.org/10.1016/j.chemosphere.2013.12.064>.

425 Kokoric, V., Theisen, J., Wilk, A., Penisson, C., Bernard, G., Mizaikoff, B., Gabriel, J.-C.P., 2018. Determining the Partial
426 Pressure of Volatile Components via Substrate-Integrated Hollow Waveguide Infrared Spectroscopy with Integrated

427 Microfluidics. *Anal. Chem.* 90, 4445-4451. <https://doi.org/10.1021/acs.analchem.7b04425>.

428 Laintz, K.E., Wai, C.M., Yonker, C.R., Smith, R.D., 1991. Solubility of fluorinated metal diethyldithiocarbamates in
429 Supercritical carbon dioxide. *J. Supercrit. Fluids* 4, 194-198. [https://doi.org/10.1016/0896-8446\(91\)90008-T](https://doi.org/10.1016/0896-8446(91)90008-T).

430 Liu, K., Li, J., Yan, S., Zhang, W., Li, Y., Han, D., 2016. A review of status of tetrabromobisphenol A (TBBPA) in China.
431 *Chemosphere* 148, 8-20. <https://doi.org/10.1016/j.chemosphere.2016.01.023>.

432 Lu, J., Han, B., Yan, H., 1999. UV-Vis spectroscopic studies of solute-solvent and solute-cosolvent interactions in supercritical
433 carbon dioxide. *Phys. Chem. Chem. Phys.* 1, 3269-3276. <https://doi.org/10.1039/A901854I>.

434 Ma, C., Yu, J., Wang, B., Song, Z., Xiang, J., Hu, S., Su, S., Sun, L., 2016. Chemical recycling of brominated flame retarded
435 plastics from e-waste for clean fuels production: a review. *Renewable and Sustainable Energy Reviews* 61, 433-450.
436 <https://doi.org/10.1016/j.rser.2016.04.020>.

437 Madras, G., Thibaud, C., Erkey, C., Akgerman, A., 1994. Modeling of supercritical extraction of organics from solid matrices.
438 *AIChE J.* 40, 777-785. <https://doi.org/10.1002/aic.690400505>.

439 Marioth, E., Bunte, G., Hardle, T., 1996. Supercritical fluid extraction of ABS-composites in order to separate organic flame
440 retardants. *Polymer Recycling(UK)* 2, 303-308.

441 Maurice, A., Theisen, J., Gabriel, J.-C.P., 2020. Microfluidic Lab-on-Chip Advances for Liquid-Liquid Extraction Process
442 Studies. *Curr. Opin. Colloid Interface Sci.* <https://doi.org/10.1016/j.cocis.2020.03.001>.

443 Nakajima, K., Kawakami, T., Ueno, T., Onishi, H., 2002. Method for treating thermoplastic resin composition containing flame
444 retardant. U. S. Patent, United States.

445 Ni, M., Xiao, H., Chi, Y., Yan, J., Buekens, A., Jin, Y., Lu, S., 2012. Combustion and inorganic bromine emission of waste
446 printed circuit boards in a high temperature furnace. *Waste Manage.* 32, 568-574.
447 <https://doi.org/10.1016/j.wasman.2011.10.016>.

448 Nimet, G., Da Silva, E.A., Palú, F., Dariva, C., dos Santos Freitas, L., Neto, A.M., Cardozo Filho, L., 2011. Extraction of

449 sunflower (*Heliantus annuus* L.) oil with supercritical CO₂ and subcritical propane: Experimental and modeling. *Chem. Eng.*
450 *J.* 168, 262-268. <https://doi.org/10.1016/j.cej.2010.12.088>.

451 Peng, S., Liang, S., Yu, M., Li, X., 2014. Extraction of polybrominated diphenyl ethers contained in waste high impact
452 polystyrene by supercritical carbon dioxide. *J. Mater. Cycles Waste Manage.* 16, 178-185. [https://doi.org/10.1007/s10163-013-](https://doi.org/10.1007/s10163-013-0169-y)
453 0169-y.

454 Poliakoff, M., Howdle, S.M., Kazarian, S.G., 1995. Vibrational spectroscopy in supercritical fluids: from analysis and
455 hydrogen bonding to polymers and synthesis. *Angewandte Chemie International Edition in English* 34, 1275-1295.
456 <https://doi.org/10.1002/anie.199512751>.

457 Sakai, S.-i., Watanabe, J., Honda, Y., Takatsuki, H., Aoki, I., Futamatsu, M., Shiozaki, K., 2001. Combustion of brominated
458 flame retardants and behavior of its byproducts. *Chemosphere* 42, 519-531. [https://doi.org/10.1016/S0045-6535\(00\)00224-1](https://doi.org/10.1016/S0045-6535(00)00224-1).

459 Sikorski, M.E., 1993. Recycling of polymeric materials from carpets and other multi-component structures by means of
460 supercritical fluid extraction. U. S. Patent, United States.

461 Sodeifian, G., Ghorbandoost, S., Sajadian, S.A., Ardestani, N.S., 2016. Extraction of oil from *Pistacia khinjuk* using
462 supercritical carbon dioxide: Experimental and modeling. *J. Supercrit. Fluids* 110, 265-274.
463 <https://doi.org/10.1016/j.supflu.2015.12.004>.

464 Sovová, H., 1994. Rate of the vegetable oil extraction with supercritical CO₂—I. Modelling of extraction curves. *Chem. Eng.*
465 *Sci.* 49, 409-414. [https://doi.org/10.1016/0009-2509\(94\)87012-8](https://doi.org/10.1016/0009-2509(94)87012-8).

466 Srinivasan, M., Smith, J., McCoy, B., 1990. Supercritical fluid desorption from activated carbon. *Chem. Eng. Sci.* 45, 1885-
467 1895. [https://doi.org/10.1016/0009-2509\(90\)87064-Y](https://doi.org/10.1016/0009-2509(90)87064-Y).

468 Stubbings, W.A., Nguyen, L.V., Romanak, K., Jantunen, L., Melymuk, L., Arrandale, V., Diamond, M.L., Venier, M., 2019.
469 Flame retardants and plasticizers in a Canadian waste electrical and electronic equipment (WEEE) dismantling facility. *Sci.*
470 *Total Environ.* 675, 594-603. <https://doi.org/10.1016/j.scitotenv.2019.04.265>.

471 Subra, P., Castellani, S., Jestin, P., Aoufi, A., 1998. Extraction of β -carotene with supercritical fluids: experiments and
472 modelling. *J. Supercrit. Fluids* 12, 261-269. [https://doi.org/10.1016/S0896-8446\(98\)00085-0](https://doi.org/10.1016/S0896-8446(98)00085-0).

473 Sunarso, J., Ismadji, S., 2009. Decontamination of hazardous substances from solid matrices and liquids using supercritical
474 fluids extraction: A review. *J. Hazard. Mater.* 161, 1-20. <https://doi.org/10.1016/j.jhazmat.2008.03.069>.

475 Suzuki, M., Nakajima, K., Onishi, H., 2002. Method for treating flame retardant resin composition. U. S. Patent, United States.

476 Tan, C.S., Liou, D.C., 1989. Modeling of desorption at supercritical conditions. *AIChE J.* 35, 1029-1031.
477 <https://doi.org/10.1002/aic.690350616>.

478 Taylor, L.T., 1996. *Supercritical fluid extraction*. Wiley New York.

479 Villanueva-Bermejo, D., Fornari, T., Calvo, M.V., Fontecha, J., Coelho, J.A., Filipe, R.M., Stateva, R.P., 2020. Application of
480 a novel approach to modelling the supercritical extraction kinetics of oil from two sets of chia seeds. *J. Ind. Eng. Chem.* 82,
481 317-323. <https://doi.org/10.1016/j.jiec.2019.10.029>.

482 Wang, H., Hirahara, M., Goto, M., Hirose, T., 2004. Extraction of flame retardants from electronic printed circuit board by
483 supercritical carbon dioxide. *J. Supercrit. Fluids* 29, 251-256. [https://doi.org/10.1016/S0896-8446\(03\)00073-1](https://doi.org/10.1016/S0896-8446(03)00073-1).

484 Wang, Z., Zhou, Q., Guo, H., Yang, P., Lu, W., 2018. Determination of water solubility in supercritical CO₂ from 313.15 to
485 473.15 K and from 10 to 50 MPa by in-situ quantitative Raman spectroscopy. *Fluid Phase Equilib.* 476, 170-178.
486 <https://doi.org/10.1016/j.fluid.2018.08.006>.

487 Xiong, P., Yan, X., Zhu, Q., Qu, G., Shi, J., Liao, C., Jiang, G., 2019. A review of environmental occurrence, fate, and toxicity
488 of novel brominated flame retardants. *Environ. Sci. Technol.* 53, 13551-13569. <https://doi.org/10.1021/acs.est.9b03159>.

489 Yu, G., Bu, Q., Cao, Z., Du, X., Xia, J., Wu, M., Huang, J., 2016. Brominated flame retardants (BFRs): a review on
490 environmental contamination in China. *Chemosphere* 150, 479-490. <https://doi.org/10.1016/j.chemosphere.2015.12.034>.

491 Zhang, C.C., Zhang, F.S., 2012. Removal of brominated flame retardant from electrical and electronic waste plastic by
492 solvothermal technique. *J. Hazard. Mater.* 221, 193-198. <https://doi.org/10.1016/j.jhazmat.2012.04.033>.

493 Zhao, Y.-B., Lv, X.-D., Ni, H.-G., 2018. Solvent-based separation and recycling of waste plastics: A review. *Chemosphere* 209,
494 707-720. <https://doi.org/10.1016/j.chemosphere.2018.06.095>.

495 Zhou, X., Guo, J., Lin, K., Huang, K., Deng, J., 2013. Leaching characteristics of heavy metals and brominated flame retardants
496 from waste printed circuit boards. *J. Hazard. Mater.* 246-247, 96-102. <https://doi.org/10.1016/j.jhazmat.2012.11.065>.

497 Zuiderveen, E., Slootweg, J.C., de Boer, J., 2020. Novel brominated flame retardants-A review of their occurrence in indoor
498 air, dust, consumer goods and food. *Chemosphere*, 126816. <https://doi.org/10.1016/j.chemosphere.2020.126816>.

499

500